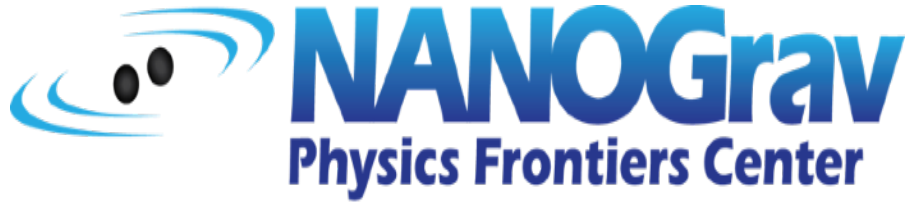


# The NANOGrav 12.5-Year Data Set: Are we nearly there?

Maura McLaughlin  
West Virginia University



# North American Nanohertz



## Observatory for GWs

Over 100 students and scientists working to characterize the GW universe at low frequencies using pulsar timing. An NSF Physics Frontiers Center since March 2015. We welcome new members and participants at meetings!

<http://nanograv.org>



# The International Pulsar Timing Array



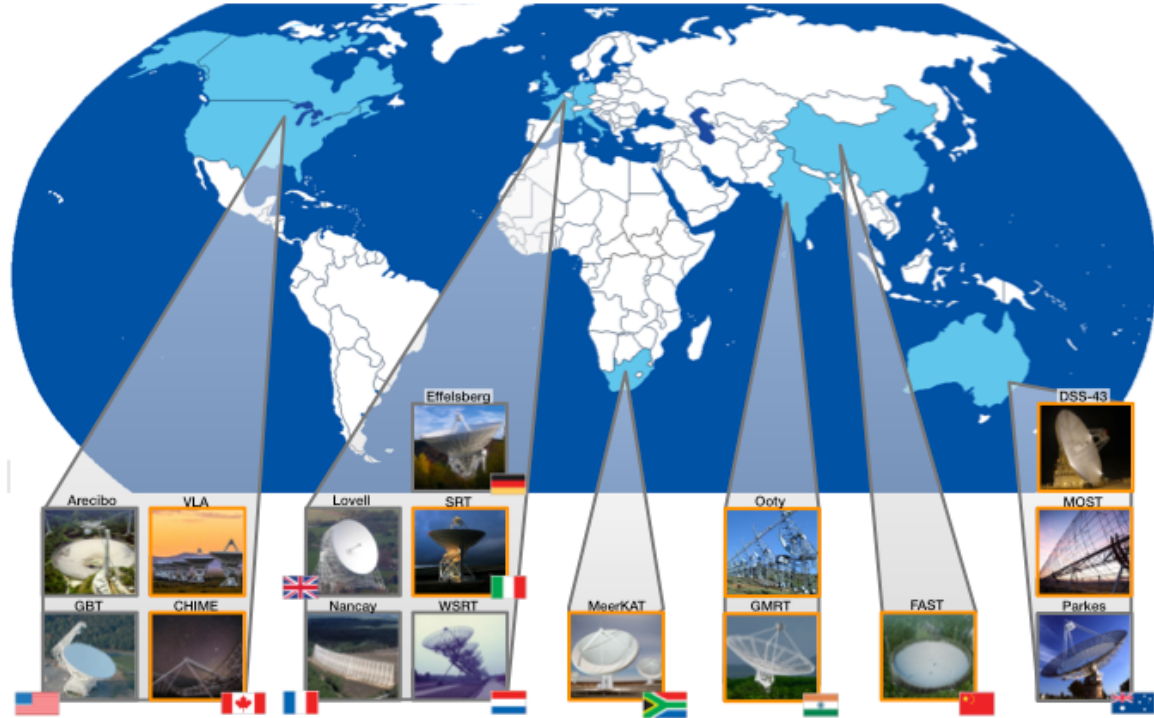
European Pulsar Timing Array



North American  
Nanohertz  
Observatory for  
Gravitational Waves



Parkes Pulsar Timing Array

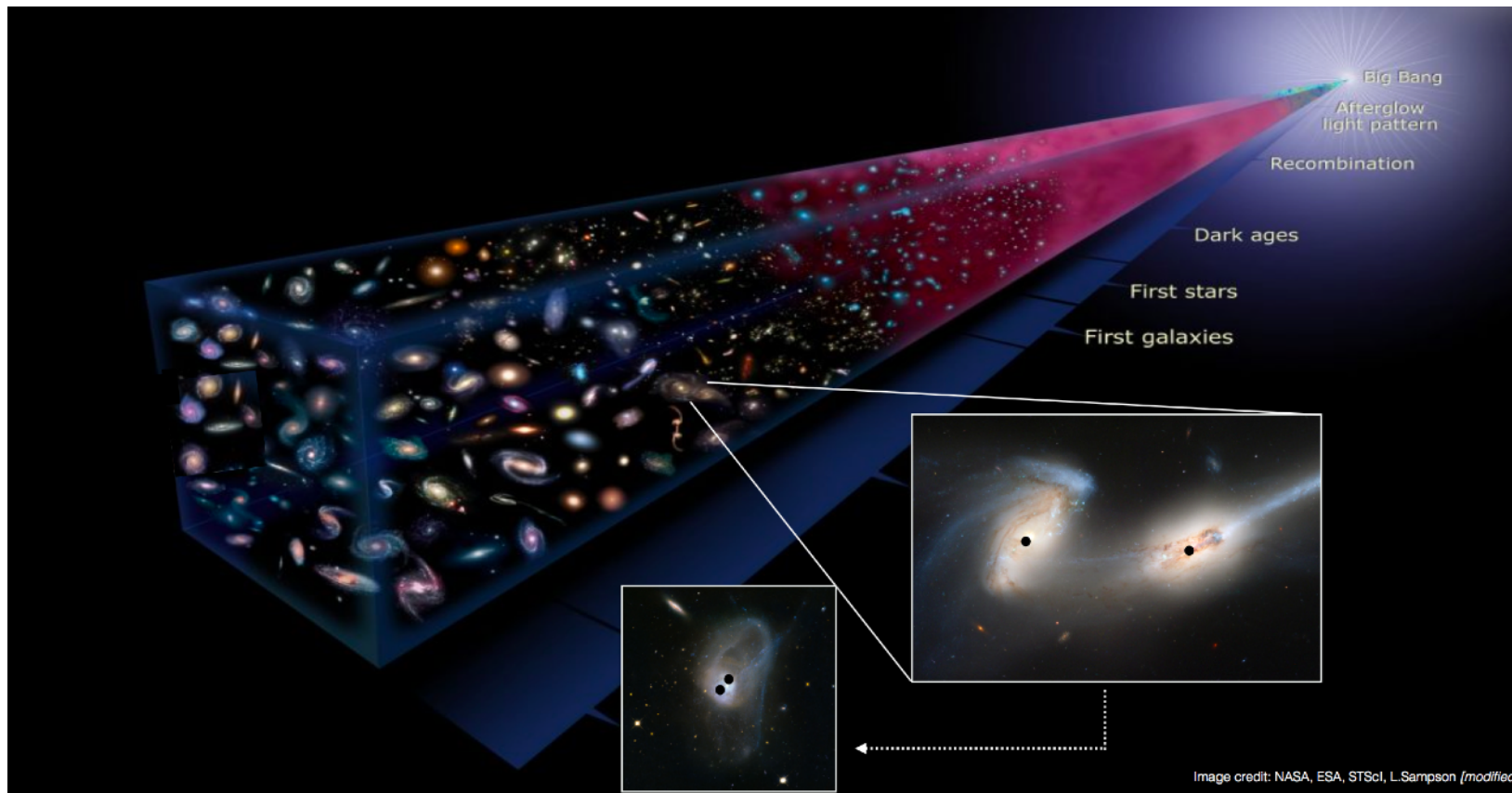


Credit: Shami Chatterjee

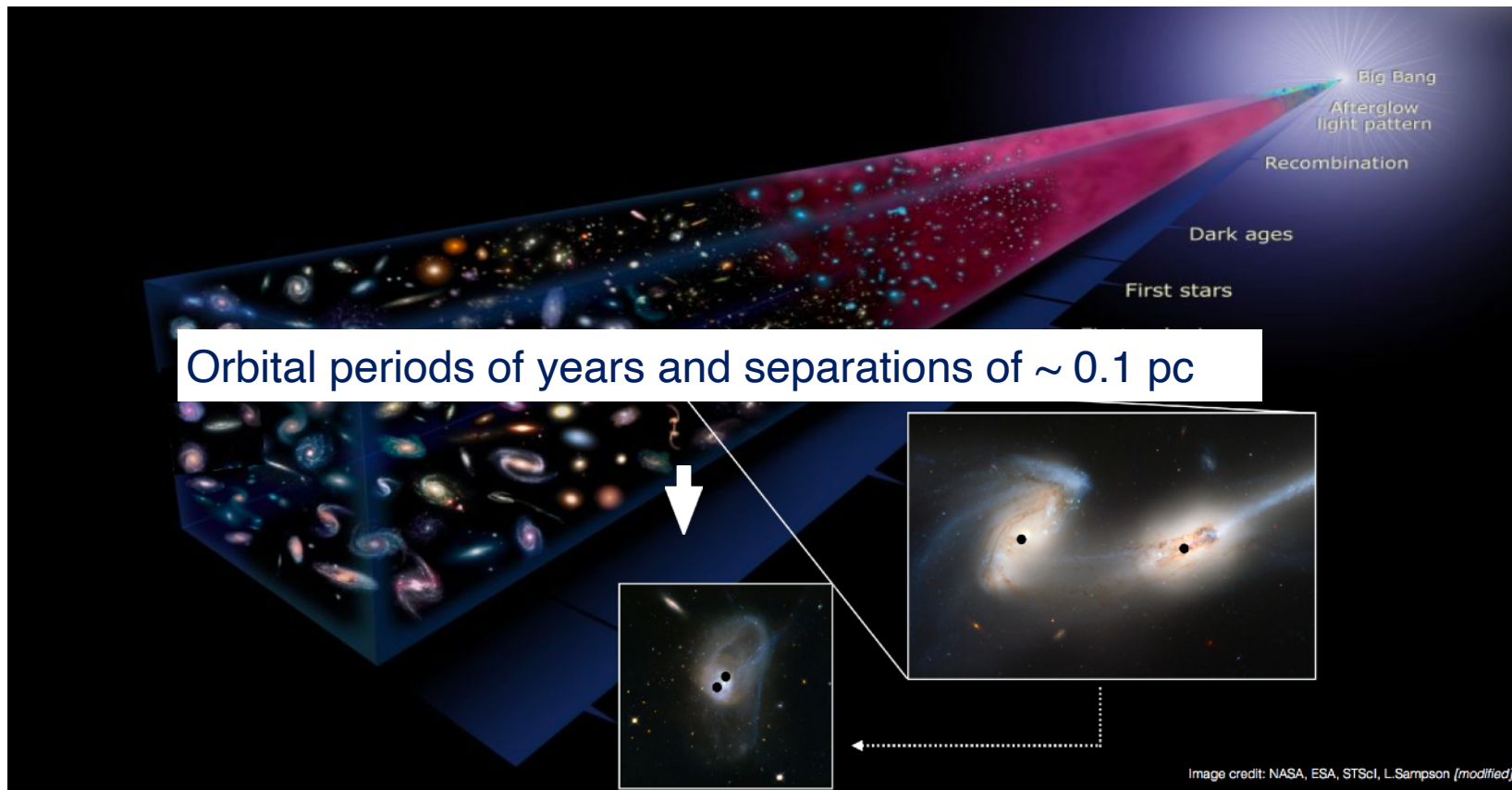
<http://ipta4gw.org>

Expanding to include data from 16 telescopes in 11 countries!

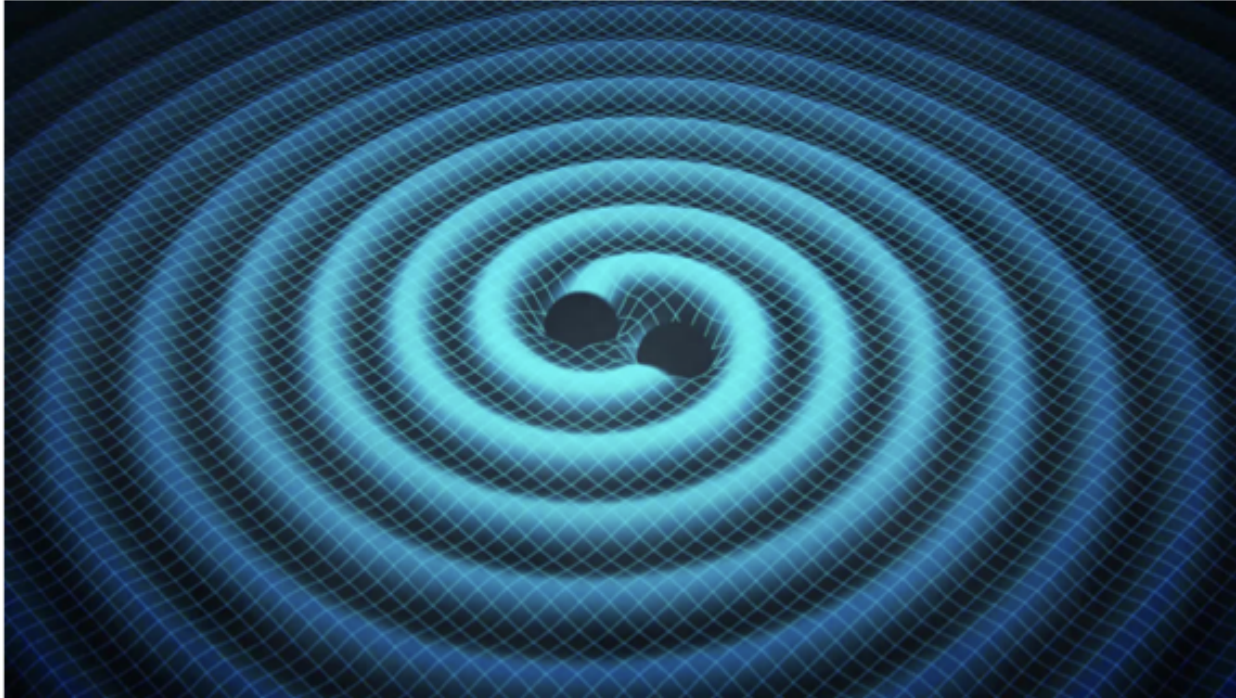
# Galaxy Evolution 101



# Galaxy Evolution 101

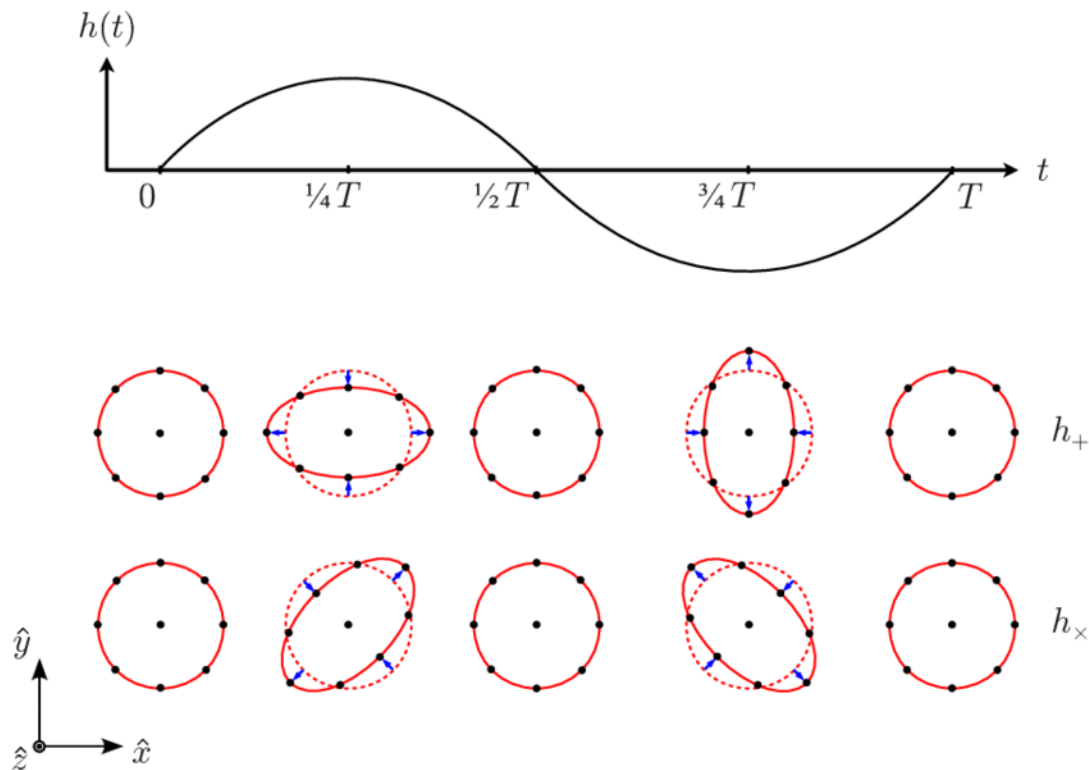


# Gravitational Waves



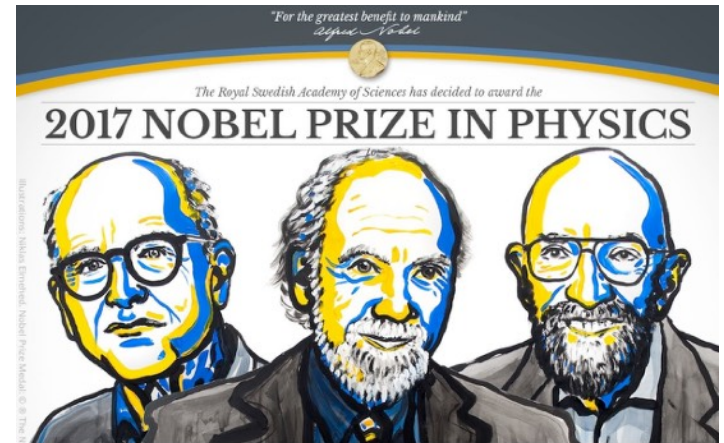
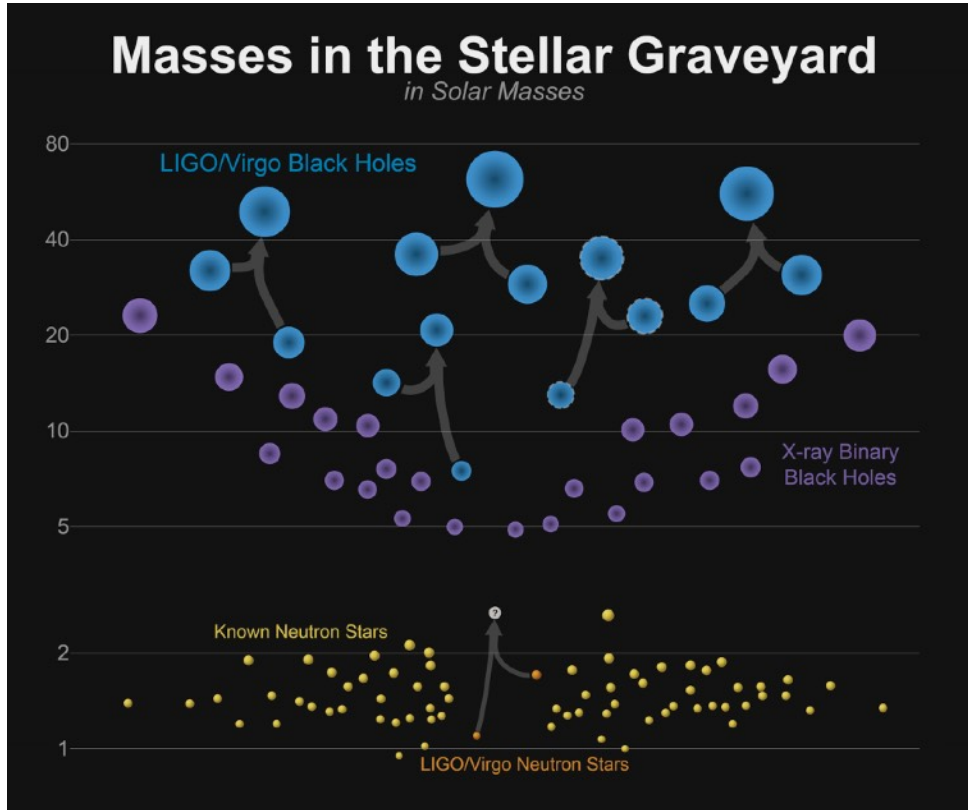
Gravitational waves (GW) are ripples in spacetime predicted by General Relativity. They are produced by massive, accelerating objects. They travel at the speed of light and are not dispersed by matter.

# Gravitational Wave Detection



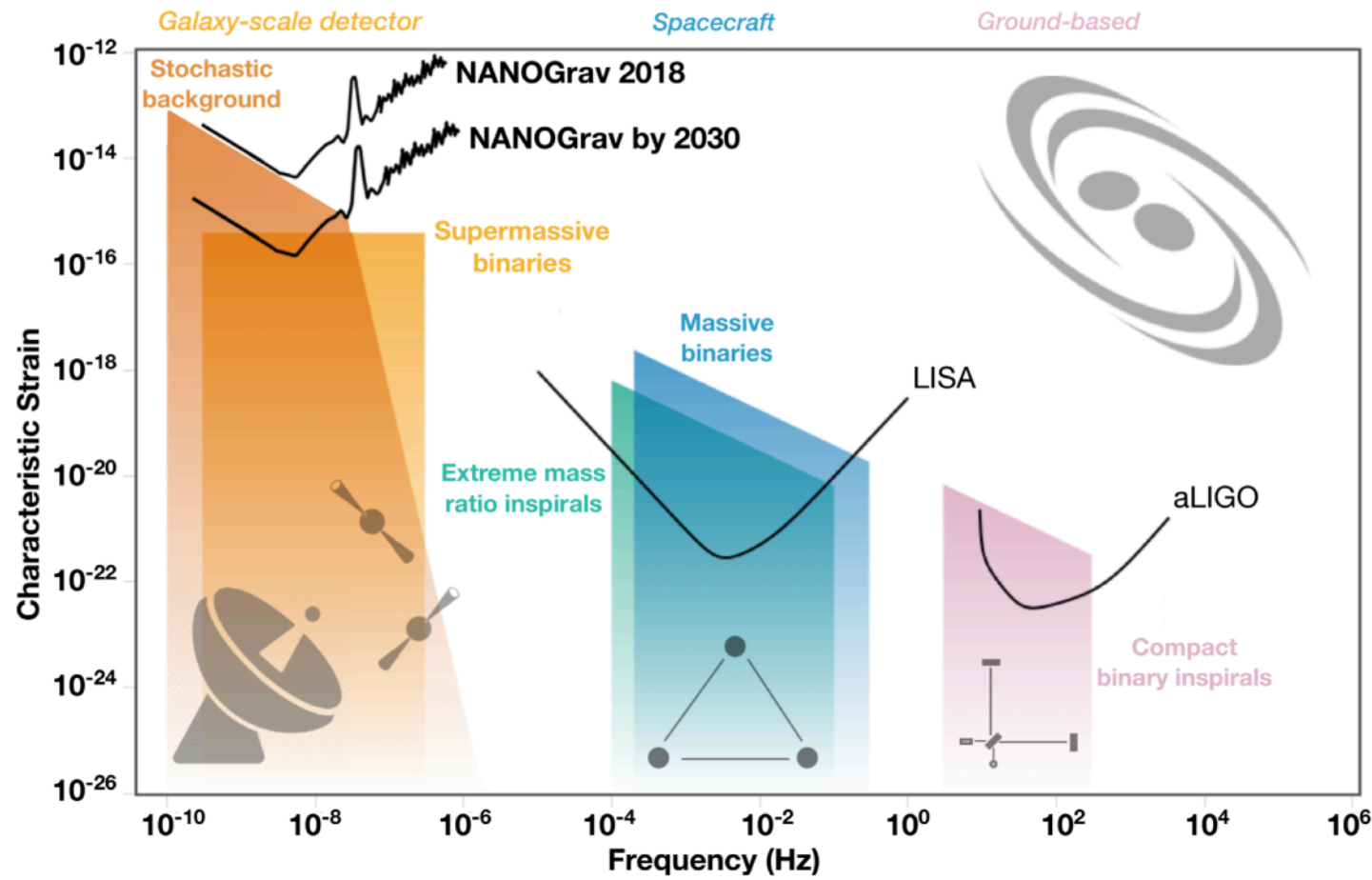
Gravitational waves change the (proper) distance between objects.

# LIGO Detection in September 2015

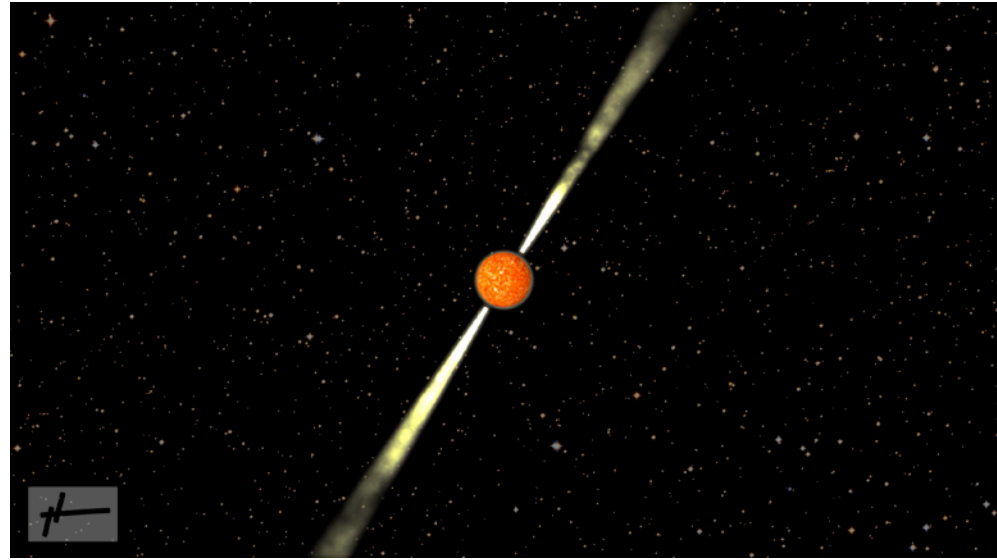
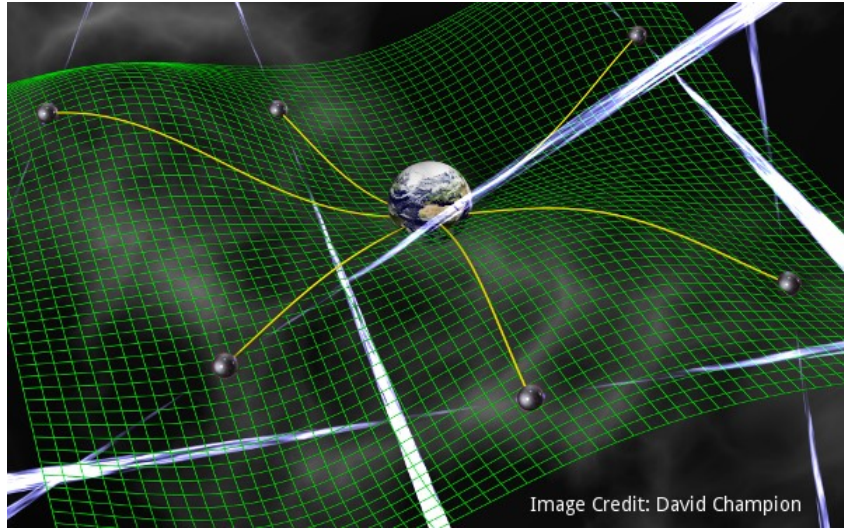




# The Gravitational Wave Spectrum



# Pulsar Timing Arrays (PTAs)

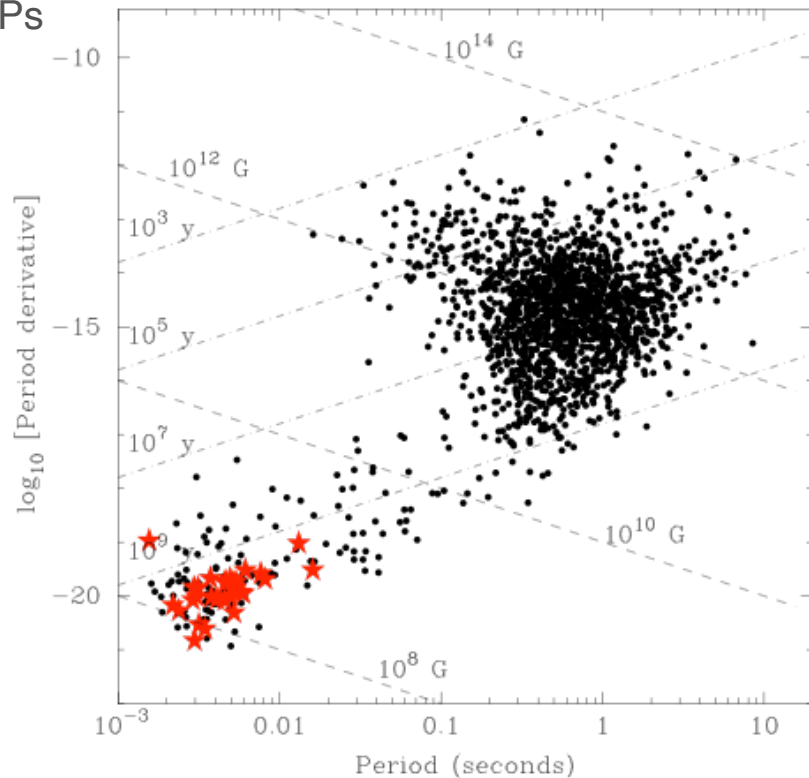
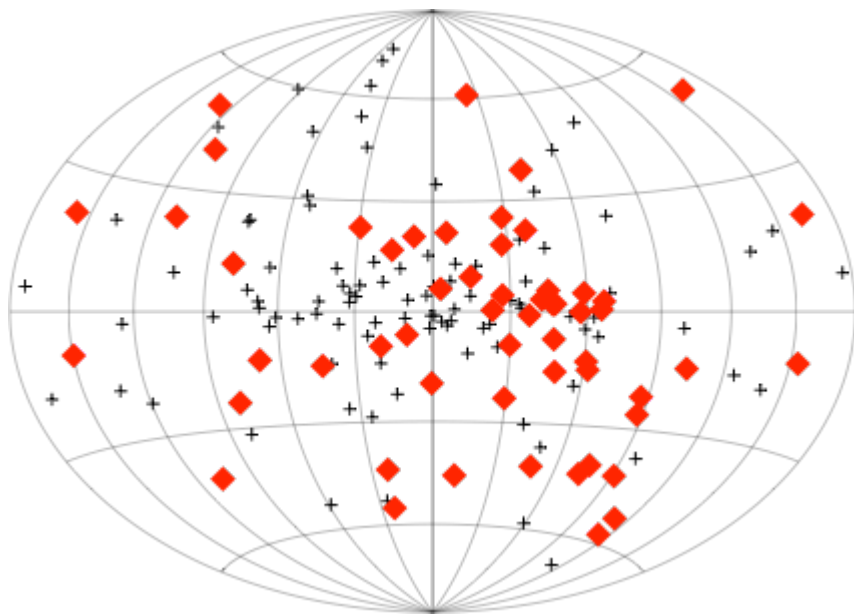


Pulsars are neutron stars born in supernova explosions.

PTA: a network of pulsars that can be used to measure various effects that produce correlations in the arrival times of pulses from the members of the array.

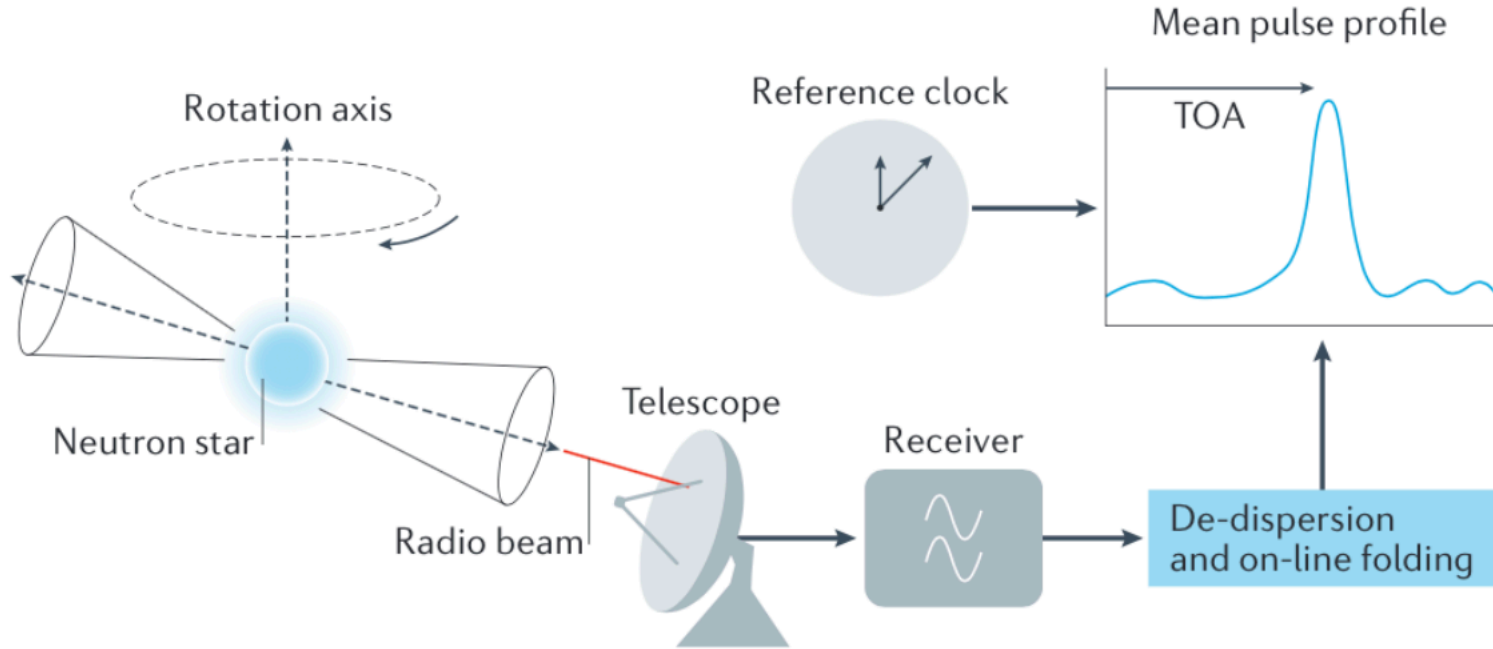
# Millisecond Pulsars (MSPs)

Out of over 2600 known pulsars, there are about 300 MSPs ( $P < 30$  ms) in our Galaxy, out of roughly 30,000-80,000 detectable. *Roughly 100 timed for PTA purposes.*



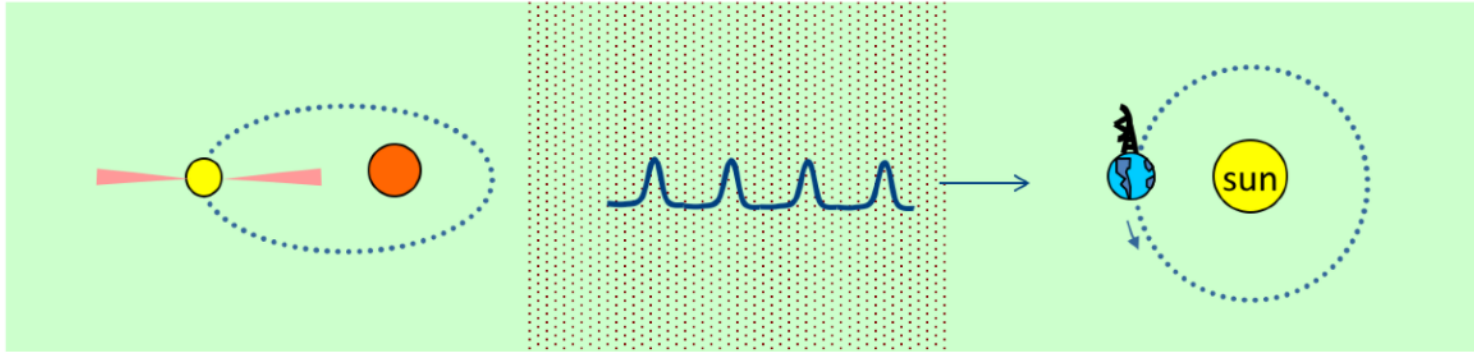
Red = part of worldwide PTA timing programs

# Pulsar Timing



Credit: "Handbook of Pulsar Astronomy", Lorimer & Kramer (2005)

# Many things affect arrival times



rotation period  
rotation period derivative  
timing noise

Keplerian orbital elements  
relativistic orbital elements

kinematic perturbations of  
orbital elements (secular  
and annual phenomena)

dispersion measure  
dispersion meas. variations

position  
proper motion  
parallax  
solar electron density

# Pulsar Timing Model

## Measured Parameters

R.A., $\alpha$ (J2000)	17:13:49.5320251(5)
decl., $\delta$ (J2000)	7:47:37.506131(12)
Spin frequency $\nu$ ( $\text{s}^{-1}$ )	218.81184385472585(6)
Spin down rate $\dot{\nu}$ ( $\text{s}^{-2}$ )	$-4.083889(4) \times 10^{-16}$
Proper motion in $\alpha$ , $\mu_\alpha = \dot{\alpha} \cos \delta$ ( $\text{mas yr}^{-1}$ )	4.9177(11)
Proper motion in $\delta$ , $\mu_\delta = \dot{\delta}$ ( $\text{mas yr}^{-1}$ )	-3.917(2)
Parallax, $\varpi$ (mas)	0.858(15)
Dispersion measure <sup>b</sup> ( $\text{pc cm}^{-3}$ )	15.9700
Orbital period, $P_b$ (day)	67.82513682426(16)
Change rate of $P_b$ , $\dot{P}_b$ ( $10^{-12} \text{ s s}^{-1}$ )	0.23(12)
Eccentricity, $e$	0.0000749394(3)
Time of periastron passage, $T_0$ (MJD)	53761.03227(11)
Angle of periastron <sup>c</sup> , $\omega$ (deg)	176.1941(6)
Projected semimajor axis, $x$ (lt-s)	32.34242243(5)
$\sin i$ , where $i$ is the orbital inclination angle	0.9672(11)
Companion mass, $M_c$ ( $M_\odot$ )	0.233(4)
Apparent change rate of $x$ , $\dot{x}$ (lt-s $\text{s}^{-1}$ )	0.00637(7)
Profile frequency dependency parameter, FD1	-0.00016317(19)
Profile frequency dependency parameter, FD2	0.0001357(3)
Profile frequency dependency parameter, FD3	-0.0000664(6)
Profile frequency dependency parameter, FD4	0.0000147(4)

## Fixed Parameters

Solar system ephemeris	DE421
Reference epoch for $\alpha$ , $\delta$ , and $\nu$ (MJD)	53729
Solar wind electron density $n_0$ ( $\text{cm}^{-3}$ )	0
Rate of periastron advance, $\dot{\omega}$ ( $\text{deg yr}^{-1}$ ) <sup>d</sup>	0.00020
Position angle of ascending node, $\Omega$ (deg) <sup>e</sup>	88.43
Red noise amplitude ( $\mu\text{s year}^{1/2}$ )	...
Red noise spectral index, $\gamma_{\text{red}}$	...

## Derived Parameters

Intrinsic period derivative, $\dot{P}_{\text{int}}$ ( $\text{s s}^{-1}$ ) <sup>h</sup>	$8.966(12) \times 10^{-21}$
Dipole magnetic field, $B$ (G) <sup>f</sup>	$2.0485(14) \times 10^8$
Characteristic age, $\tau_c$ (year) <sup>g</sup>	$8.076(11) \times 10^9$
Pulsar mass, $M_{\text{PSR}}$ ( $M_\odot$ )	0.97(3)

Spin and spin-down

Astrometric

Interstellar medium

Binary

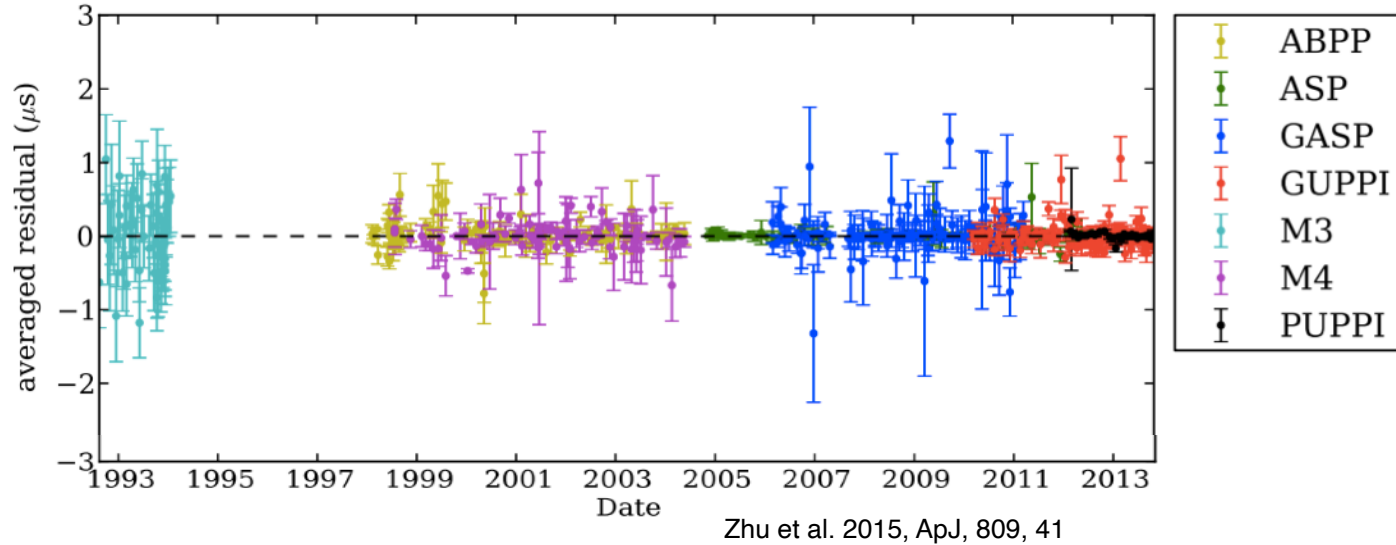
Pulsar profile evolution

Red and white noise

Zhu et al. 2015, ApJ, 809, 41

# Timing Residuals

Model – Measured  
Barycentric TOAs

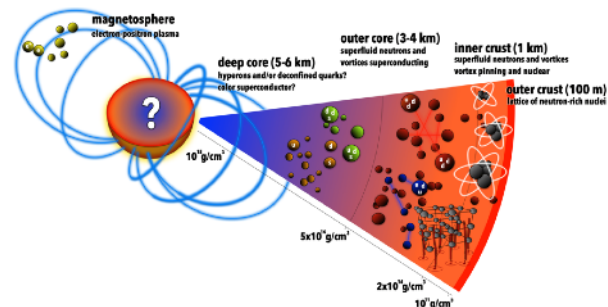


PSR J1713+0747 ( $P=4.57$  ms).

TOAs measured to tens of ns - RMS  $\sim 70$  ns over *decades* timescales.

# Sources of Noise in PTA Data

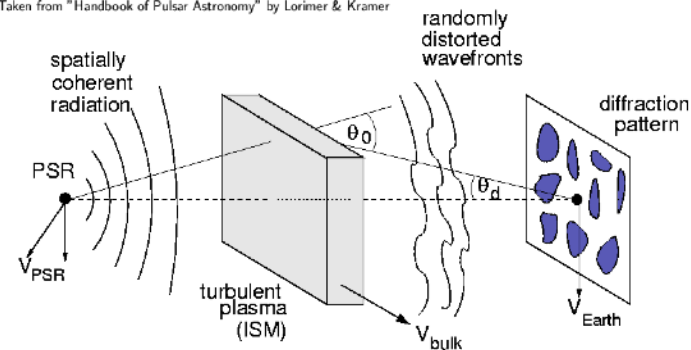
	Noise source	Achromatic?	Correlated in time?	Correlated in space?
Intrinsic	Pulsar rotational irregularities	✓	✓	✗
	Pulse jitter	✓	✗	✗
Extrinsic	Scattering and dispersion measure variations	✗	✓	✗
	Planetary ephemerides	✓	✓	✓
	Clock errors/offsets	✓	✓	✗



Watts et al. 2015, arXiv: 1501.00042



Taken from "Handbook of Pulsar Astronomy" by Lorimer & Kramer





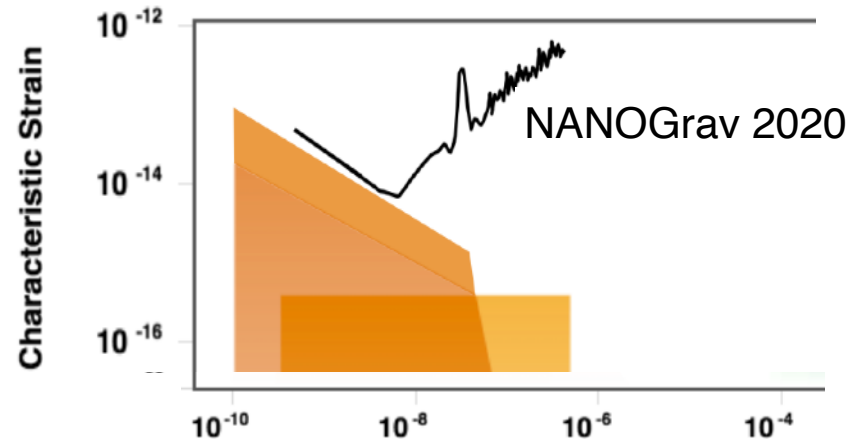
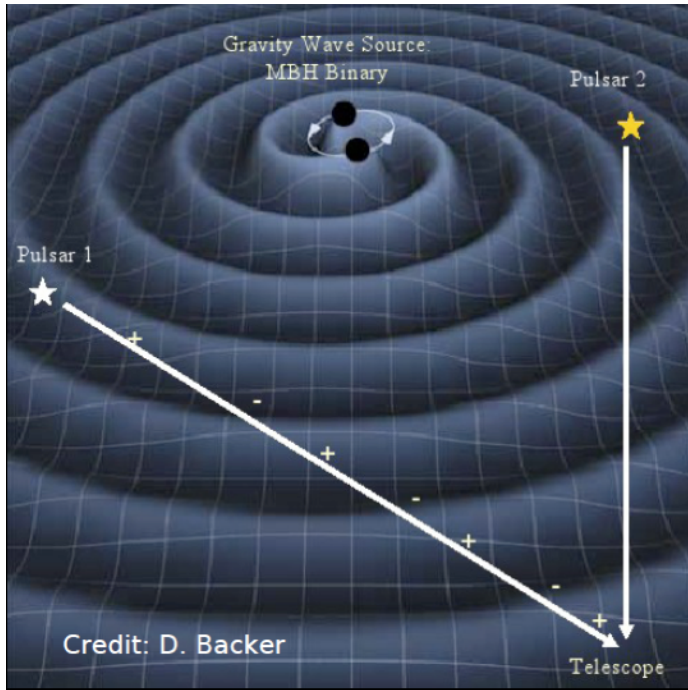
# Detection Big Picture

$f \sim 1/\text{weeks to 1/years } (10^{-6} - 10^{-9} \text{ Hz})$

The induced residual  $\Delta t \sim h/f$  and will have pulsar and Earth terms.

$h_{\text{min}} \sim \sigma_{\text{rms}}/T \sim 200 \text{ ns}/10 \text{ years} \sim 10^{-15}$

$\lambda_{\text{gw}} \sim 1\text{-}10 \text{ yr}; D_{\text{psr}} \sim 1000 \text{ yr}$



# PTA Sources

For a binary system,

$$h \simeq 10^{-17} M_8^{5/3} f_{\text{yr}^{-1}}^{2/3} D_{\text{Gly}}^{-1} \frac{q}{(1+q)^2}$$

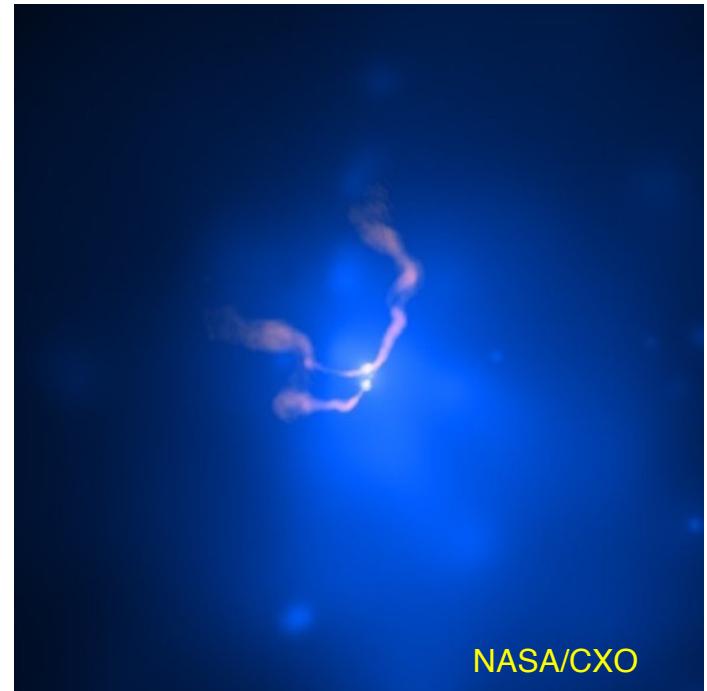
$$\tau = 10^6 M_8^{-5/3} f_{\text{yr}^{-1}}^{-8/3} \frac{(1+q)^2}{q} \text{yr}$$

For a stochastic background,

$$h_c(f) = A_{\text{GWB}} \left( \frac{f}{\text{yr}^{-1}} \right)^\alpha$$

$$\alpha = -2/3$$

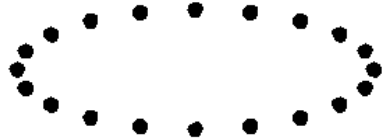
(under the simplest assumptions)



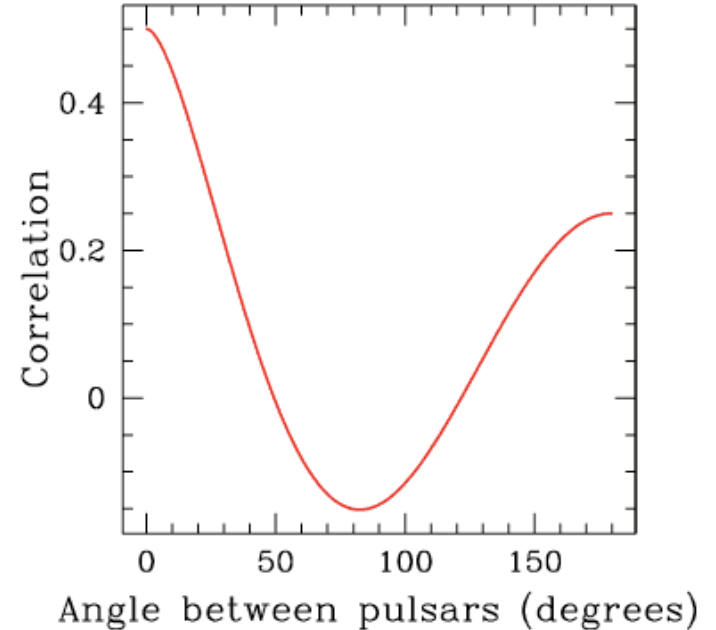
Will look like correlated  
 RED noise in our data.

# The Expected Correlation

Expected correlation of residuals for pairs of pulsars versus angular separation on sky. Pulsar terms uncorrelated. Earth terms correlated.



Clock errors monopole.  
Ephemeris errors dipole.  
GWs quadrupole.



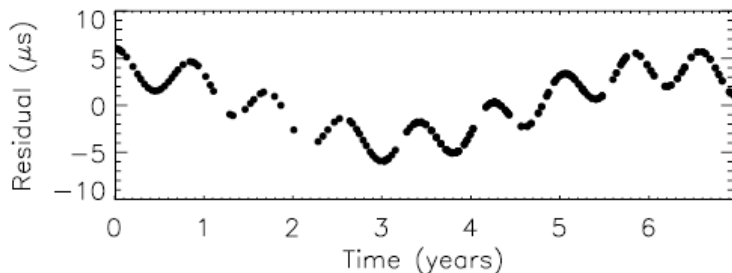
Hellings & Downs, 1983, ApJ, 265, L39

# Can we distinguish GWs from noise?

	Noise source	Achromatic?	Correlated in time?	Correlated in space?	Quadrupolar?
Intrinsic	Pulsar rotational irregularities	✓	✓	✗	✗
	Pulse jitter	✓	✗	✗	✗
Extrinsic	Scattering and dispersion measure variations	✗	✓	✗	✗
	Planetary ephemerides	✓	✓	✓	✗
	Clock errors/offsets	✓	✓	✗	✗
	<b>GW background</b>	✓	✓	✓	✓

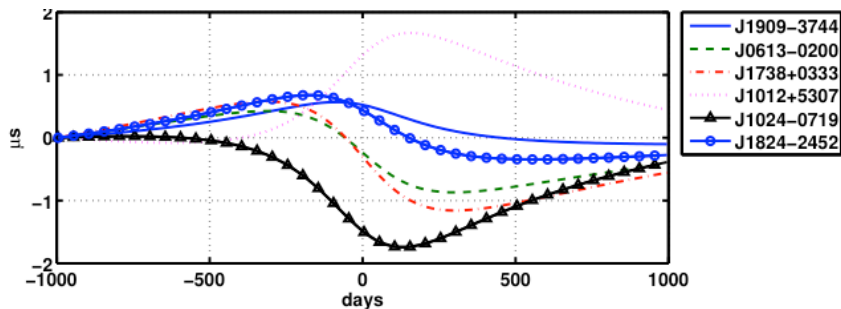
**Yes!**

# And detect single sources through continuous wave and burst searches



Jenet et al. 2004, ApJ, 606, 799

50 billion solar mass binary with period of one year at 100 Mpc (3C66B).



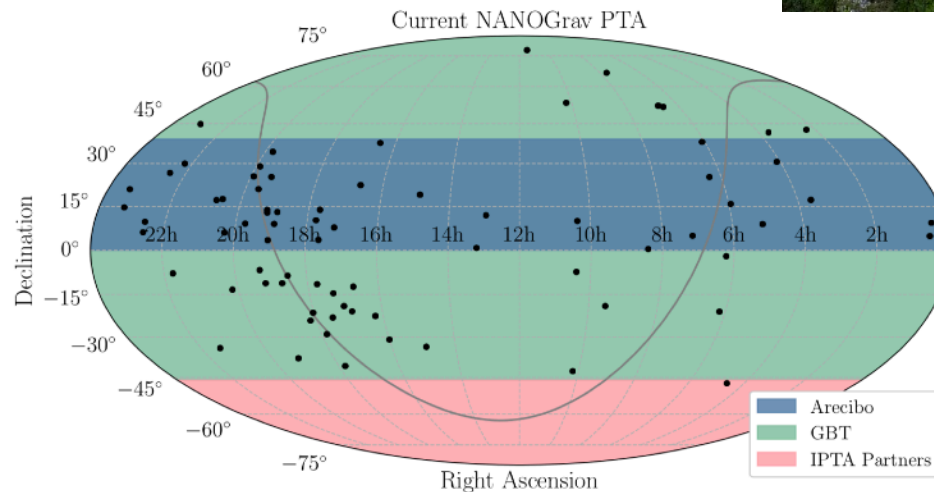
Finn & Lommen, ApJ, 2000, 718 1400

Parabolic encounter of two billion solar mass black holes at 20 Mpc.



# NANOGrav's Observing Program

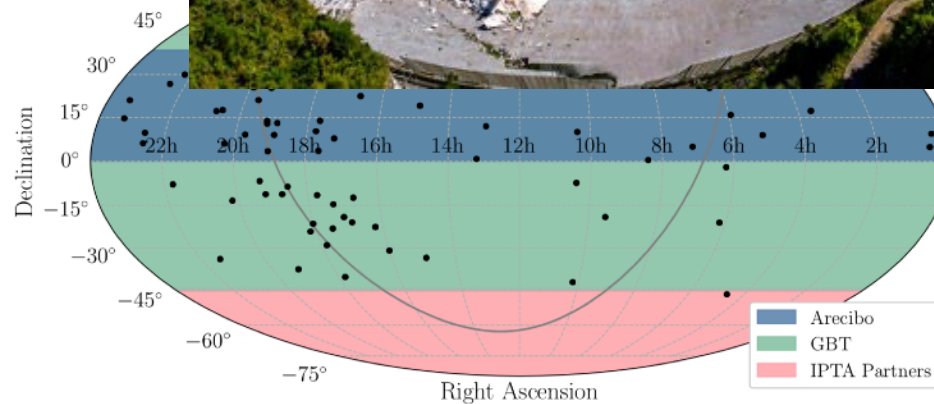
We have been observing 79 MSPs at two frequencies (from 800 MHz to 3 GHz) every one to four weeks for roughly 20-30 min using Arecibo (41 MSPs, 5 weekly), the GBT (39 MSPs, 2 weekly), and the VLA (7 MSPs).



The NANOGrav Collaboration, 2018, ApJS, 235, 37

# NANOGrav's Observing Program

We observe 79 MSPs at two frequencies (from one to four weeks for roughly 20-30 min using weekly), the GBT (39 MSPs, 2 weekly), and the



The NANOGrav Collaboration, 2018, ApJS, 235, 37

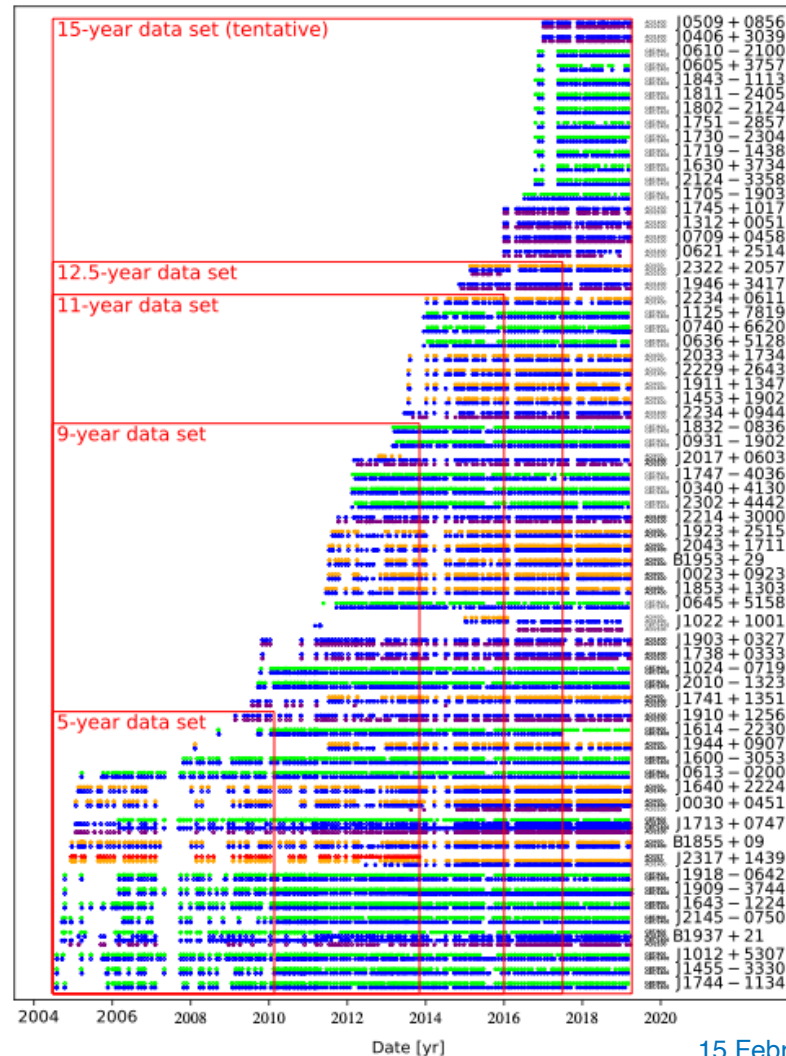


# NANOGrav's Data Releases

We release data and carry out new gravitational wave searches every ~two years.

Publicly available at  
<http://data.nanograv.org>

The NANOGrav Collaboration, 2018, ApJS, 235, 37  
The NANOGrav Collaboration, 2021, APSS, 252, 48  
The NANOGrav Collaboration, 2021, APSS, 252, 53



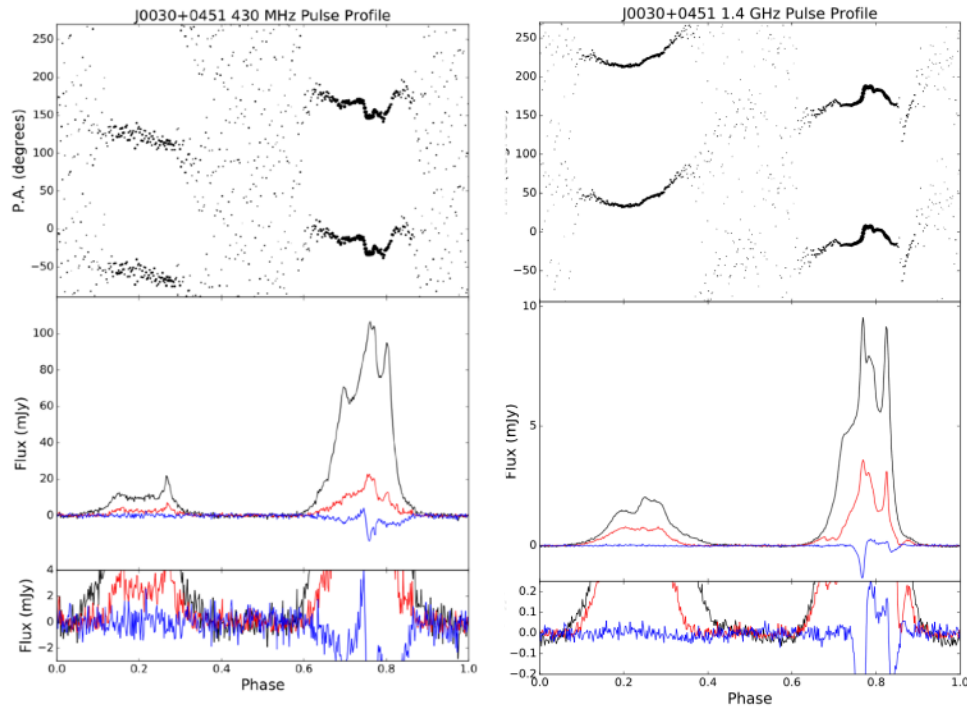
# NANOGrav's Data Releases

Contain full Stokes profiles, per frequency times of arrival, and timing parameter files

```

guppi_57378_J0613-0200_0006.11y.x.ff 869.218018 57378.2467338787318 0.624 gbt -fe Rcvr_800 -be GUPPI
guppi_57378_J0613-0200_0006.11y.x.ff 872.343018 57378.246733896636763 1.697 gbt -fe Rcvr_800 -be GUPPI
guppi_57378_J0613-0200_0006.11y.x.ff 875.396973 57378.246733879571675 0.792 gbt -fe Rcvr_800 -be GUPPI
guppi_57378_J0613-0200_0006.11y.x.ff 878.593018 57378.246733897356721 0.570 gbt -fe Rcvr_800 -be GUPPI
guppi_57378_J0613-0200_0006.11y.x.ff 881.718018 57378.246733888282248 0.539 gbt -fe Rcvr_800 -be GUPPI
guppi_57378_J0613-0200_0006.11y.x.ff 884.843018 57378.246733898813908 0.772 gbt -fe Rcvr_800 -be GUPPI
guppi_57378_J0613-0200_0006.11y.x.ff 887.968018 57378.246733882110973 0.745 gbt -fe Rcvr_800 -be GUPPI
guppi_57378_J0613-0200_0006.11y.x.ff 891.093018 57378.246733991030715 0.713 gbt -fe Rcvr_800 -be GUPPI
guppi_57378_J0613-0200_0006.11y.x.ff 894.218018 57378.246733884676130 1.639 gbt -fe Rcvr_800 -be GUPPI
guppi_57378_J0613-0200_0006.11y.x.ff 897.343018 57378.246733993905295 1.686 gbt -fe Rcvr_800 -be GUPPI
guppi_57378_J0613-0200_0006.11y.x.ff 900.468018 57378.246733887895996 1.125 gbt -fe Rcvr_800 -be GUPPI
guppi_57378_J0613-0200_0006.11y.x.ff 903.593018 57378.246733907517509 1.969 gbt -fe Rcvr_800 -be GUPPI

```



Gentile et al., 2018, ApJ, 862, 47

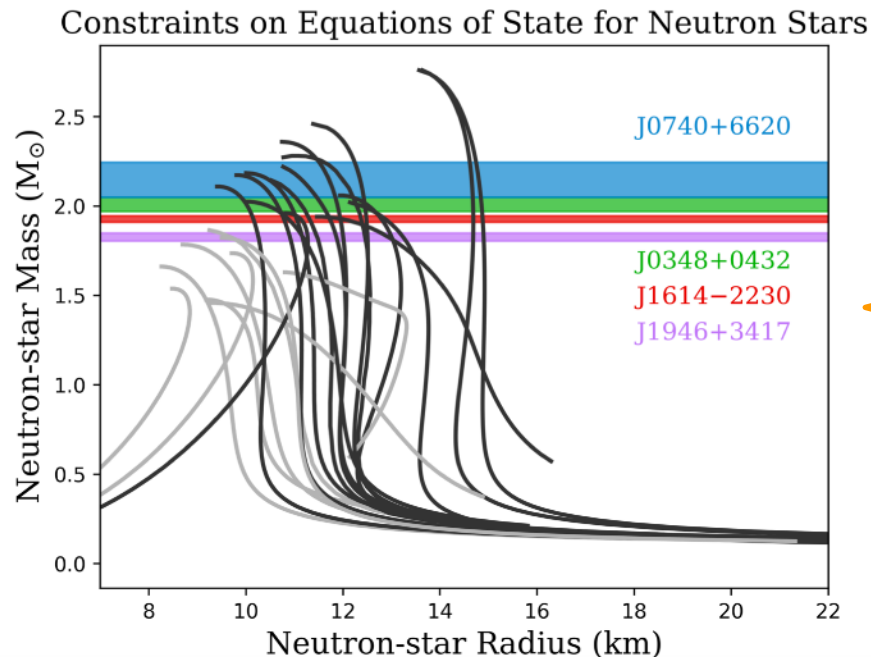
Table 1: PSR J0740+6620 Best-Fit Parameters

Pulsar name	J0740+6620
Dates of Observations (MJD)	56640 – 58462
Number of TOAs	7419
Measured Quantities	
Ecliptic longitude, $\lambda$ (degrees)	103.75913607(1)
Ecliptic latitude, $\beta$ (degrees)	44.10248468(2)
Epoch of position & period (MJD)	57551.0
Proper motion in ecliptic longitude ( $\text{mas yr}^{-1}$ )	-2.75(3)
Proper motion in ecliptic latitude ( $\text{mas yr}^{-1}$ )	-32.43(4)
Parallax (mas)	0.5(3)
Spin frequency, $\nu$ (Hz)	346.5319964932129(6)
Spin frequency derivative, $\dot{\nu}$ ( $\text{s}^{-2}$ )	$-1.46389(2) \times 10^{-15}$
Dispersion measure, DM ( $\text{pc cm}^{-3}$ )*	14.961787
Profile frequency dependency parameter, FD1	$-1.17(4) \times 10^{-5}$
Binary model	ELL1
Projected semi-major axis of orbit, $x$ (lt-s)	3.9775561(2)
Binary orbital period, $P_b$ (days)	4.7669446191(1)
Epoch of ascending node, TASC (MJD)	57552.08324415(2)
EPS1 (first Laplace-Lagrange parameter), $e \sin \omega$	$-5.70(4) \times 10^{-6}$
EPS2 (second Laplace-Lagrange parameter), $e \cos \omega$	$-1.89(3) \times 10^{-6}$
Sine of inclination angle $i$	0.9990(2)
Companion mass, $m_c$ ( $M_\odot$ )	0.258(8)

Cromartie et al., 2019, Nature Astronomy, 439

# Lots of other cool science!

Our timing data can be used for neutron star mass measurements, tests of general relativity, studies of the interstellar medium and the solar wind, and Galactic astrometry.



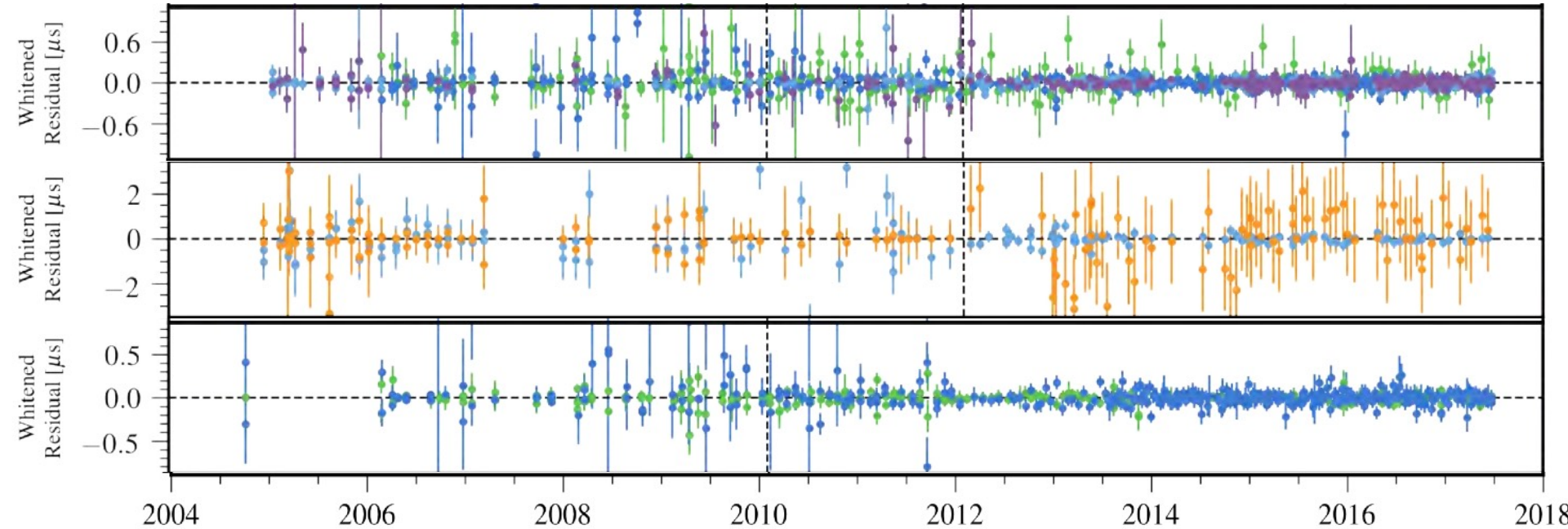
Fonseca et al., 2019, arXiv:1903.0819

Table 1: PSR J0740+6620 Best-Fit Parameters

Measured Quantities	
Pulsar name	J0740+6620
Dates of Observations (MJD)	56640 – 58462
Number of TOAs	7419
Measured Quantities	
Ecliptic longitude, $\lambda$ (degrees)	103.75913607(1)
Ecliptic latitude, $\beta$ (degrees)	44.10248468(2)
Epoch of position & period (MJD)	57551.0
Proper motion in ecliptic longitude ( $\text{mas yr}^{-1}$ )	-2.75(3)
Proper motion in ecliptic latitude ( $\text{mas yr}^{-1}$ )	-32.43(4)
Parallax (mas)	0.5(3)
Spin frequency, $\nu$ (Hz)	346.5319964932129(6)
Spin frequency derivative, $\dot{\nu}$ ( $\text{s}^{-2}$ )	$-1.46389(2) \times 10^{-15}$
Dispersion measure, DM ( $\text{pc cm}^{-3}$ )*	14.961787
Profile frequency dependency parameter, FD1	$-1.17(4) \times 10^{-5}$
Binary model	ELL1
Projected semi-major axis of orbit, $x$ (lt-s)	3.9775561(2)
Binary orbital period, $P_b$ (days)	4.7669446191(1)
Epoch of ascending node, TASC (MJD)	57552.08324415(2)
EPS1 (first Laplace-Lagrange parameter), $e \sin \omega$	$-5.70(4) \times 10^{-6}$
EPS2 (second Laplace-Lagrange parameter), $e \cos \omega$	$-1.89(3) \times 10^{-6}$
Sine of inclination angle $i$	0.9990(2)
Companion mass, $m_c$ ( $M_{\odot}$ )	0.258(8)

Cromartie et al., 2019, Nature Astronomy, 439

Residuals = model - measured times of arrival (TOAs)

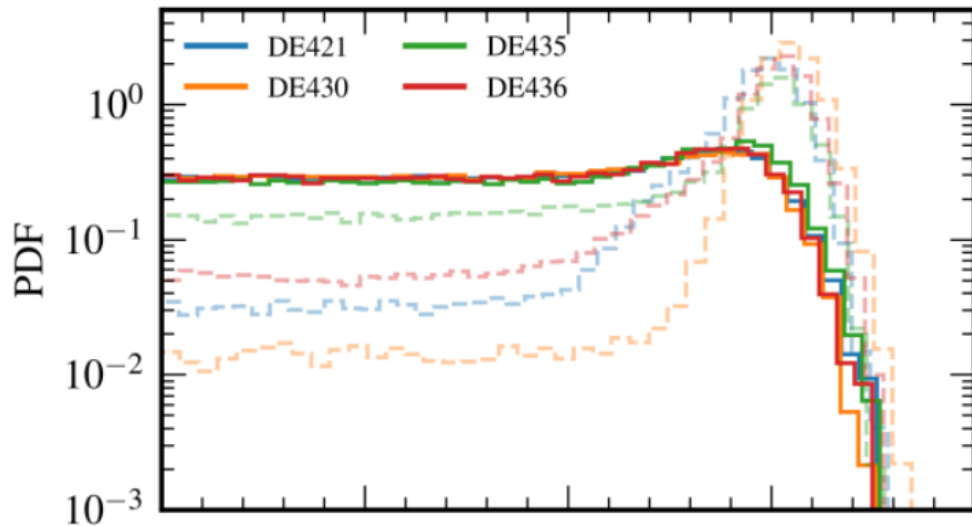


The NANOGrav Collaboration, 2021, APSS, 252, 48

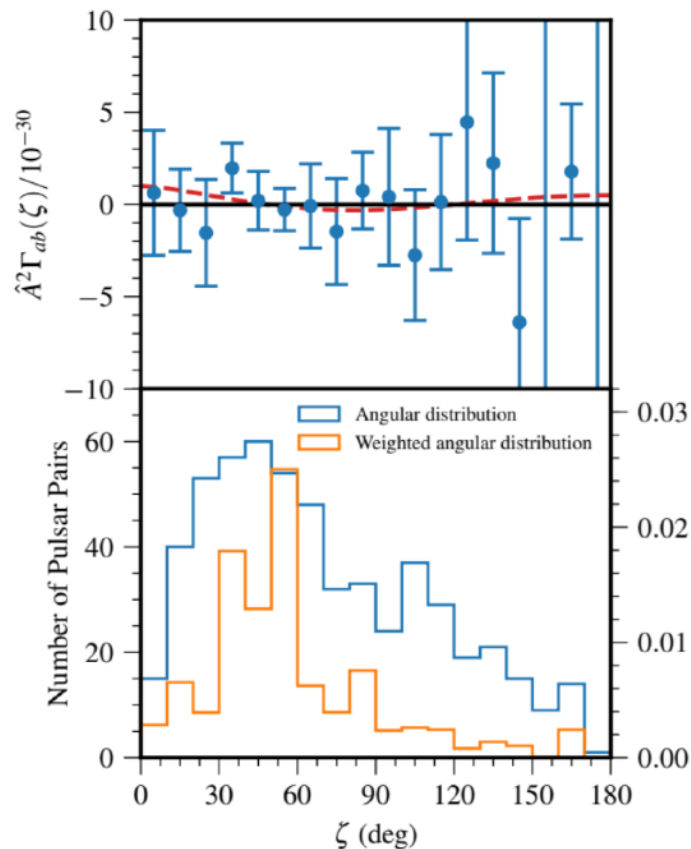
We search residuals for red noise (stochastic background), sine waves (single sources), or step functions (bursts with memory) that are correlated among pulsars.

# Eleven-year Stochastic Background Analysis

No detection yet!



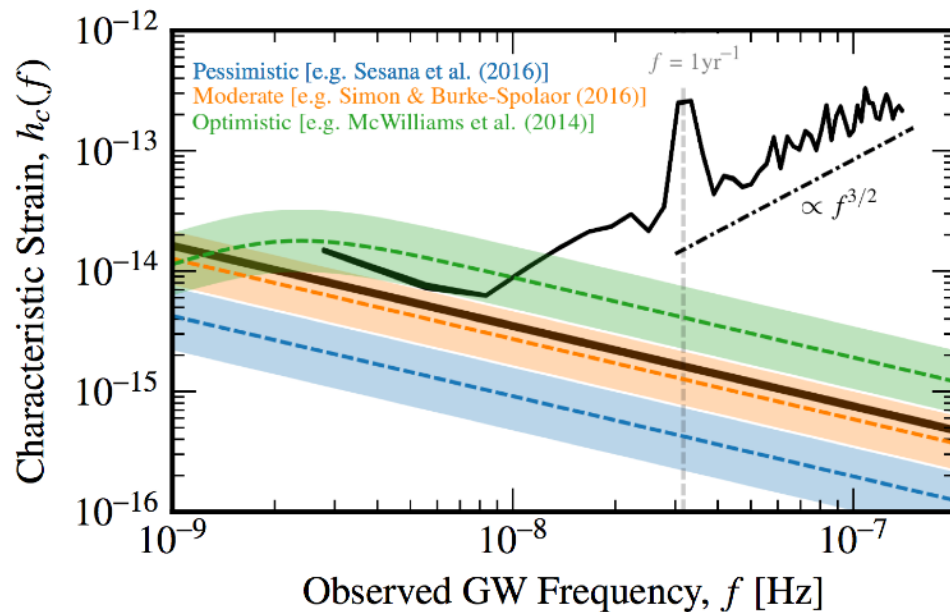
Developed new Bayesian methods to model Solar System ephemeris uncertainties



The NANOGrav Collaboration, 2018, ApJ, 859, 47

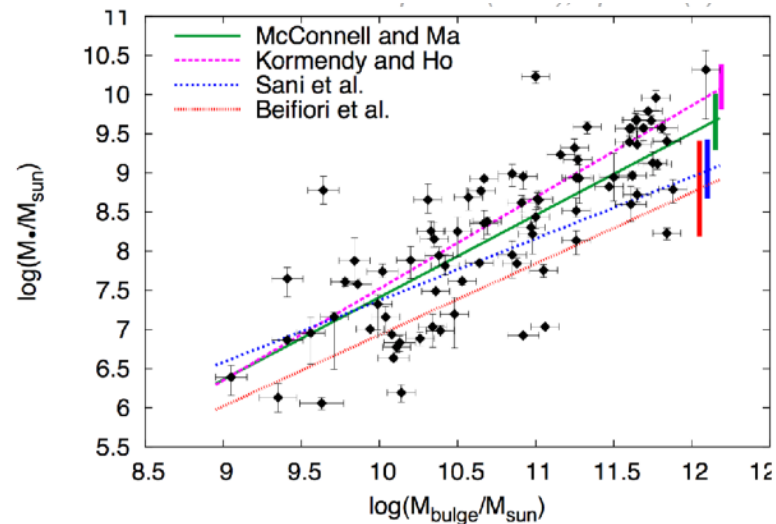
# Our limit can rule out SMBBH formation and evolution models

Can constrain astrophysical effects:  
stellar hardening  
circumbinary disk interaction  
binary eccentricity



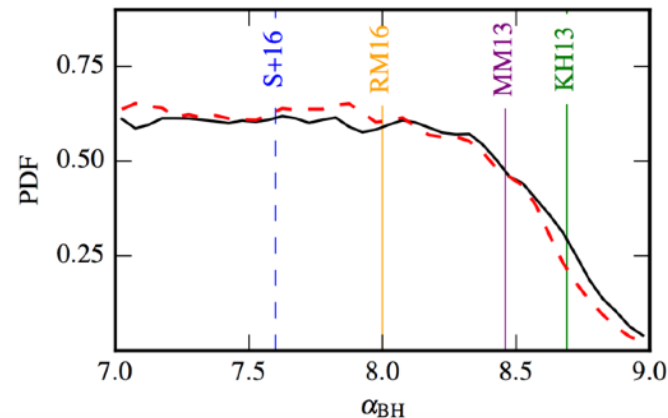
The NANOGrav Collaboration, 2018, ApJ, 859, 47

# And make robust astrophysical constraints



Simon & Burke-Spolaor, 2016, ApJ, 826, 1

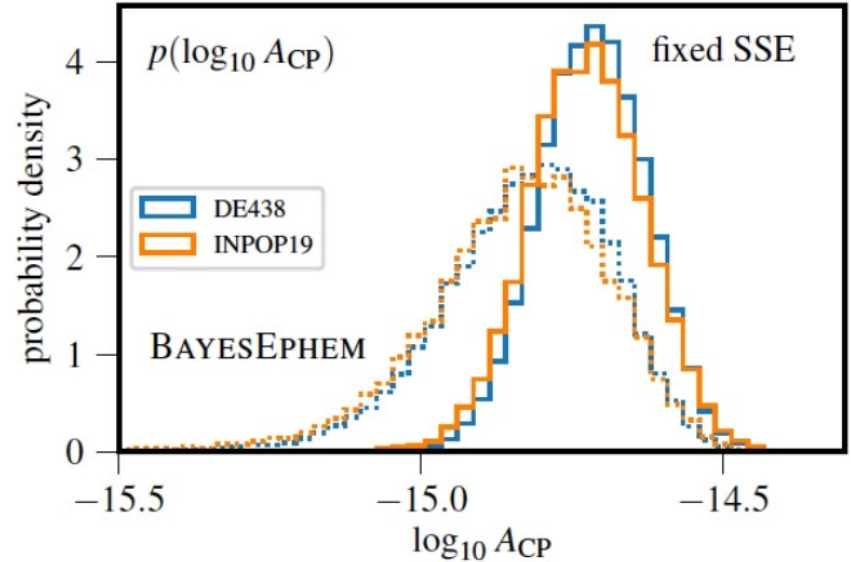
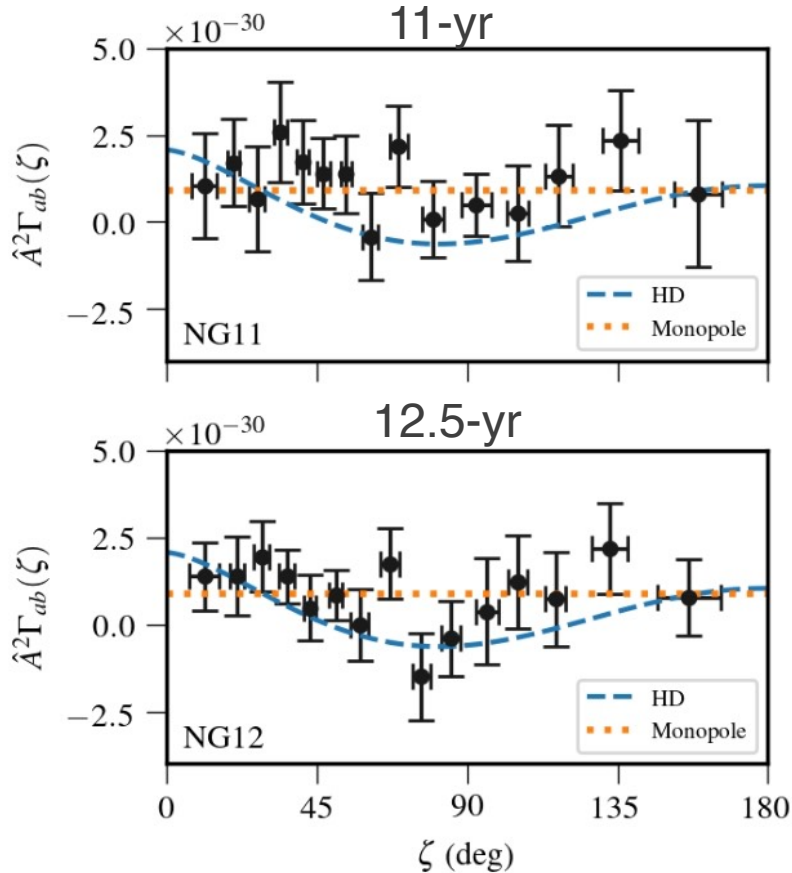
$$\log_{10} M_{\bullet} = \alpha + \beta \log_{10} \left( \frac{M_{\text{bulge}}}{10^{11} M_{\odot}} \right)$$



The NANOGrav Collaboration, 2018, ApJ, 859, 47

Can rule out astrophysical parameter space and place constraints on eccentricity, galaxy-bulge mass relationship, and galactic core mass density.

# 12.5-Yr Results

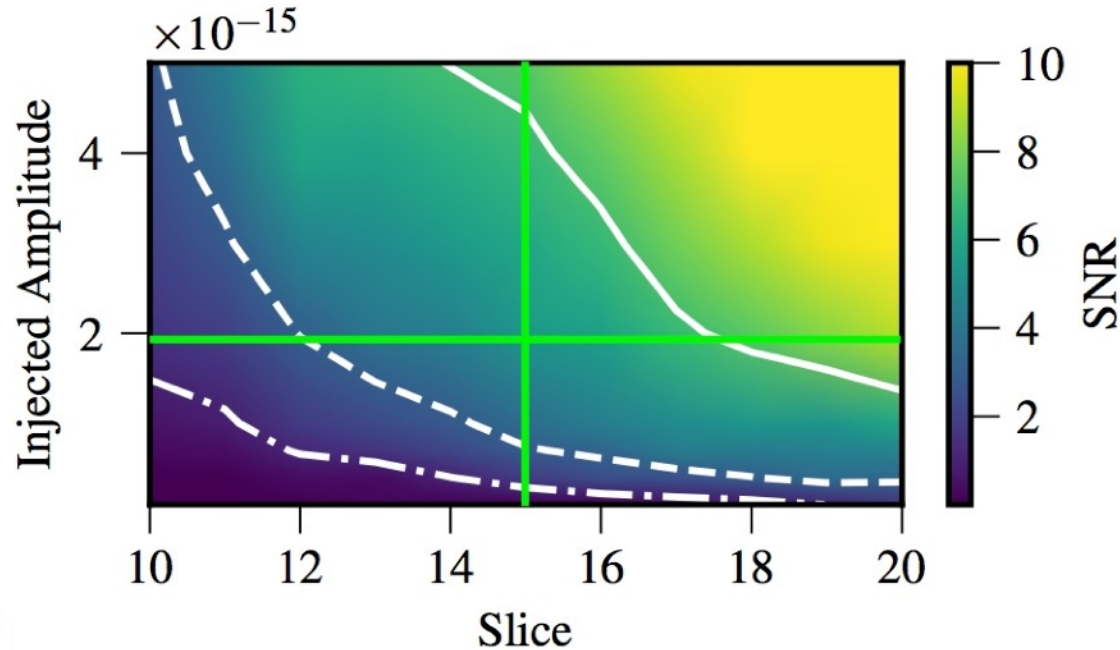


Strong common red noise process among all pulsars. But cannot yet distinguish quadrupolar signature.

The NANOGrav Collaboration, 2020, ApJ, 905, 34



# When will we get there?



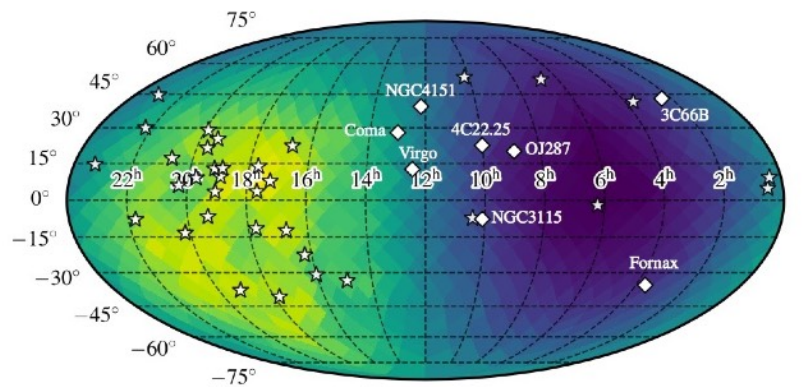
We expect evidence at a SNR of 4-7 in our upcoming 15-yr data set.

Measurement of amplitude and spectrum will allow unique constraints on galaxy formation and evolution.

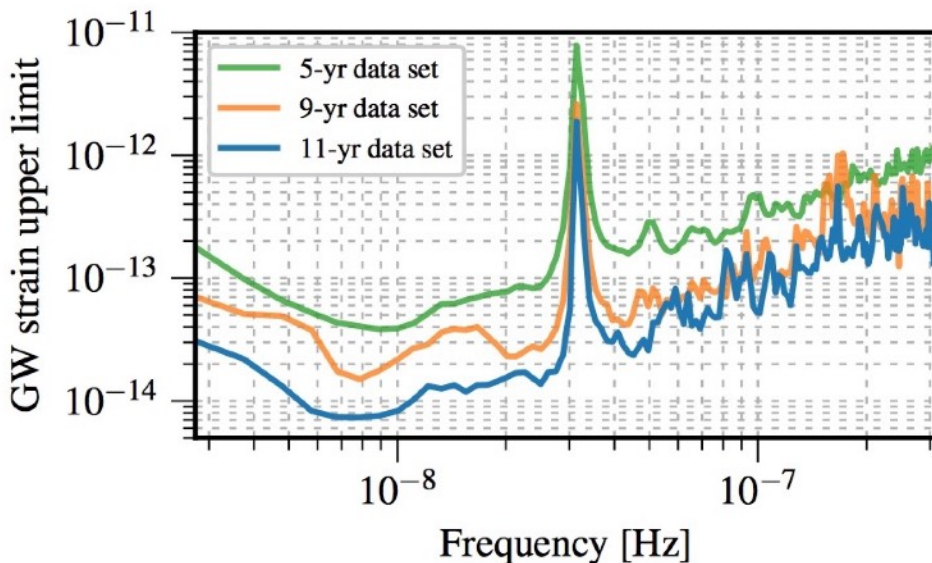
# Eleven-year Continuous Wave Results

Sky-averaged limit of  $7 \times 10^{-15}$  ( $f=8$  nHz)

Highly direction dependent!



$$D_{95} \times \left( \frac{\mathcal{M}}{10^9 M_{\odot}} \right)^{5/3} \times \left( \frac{f}{8 \times 10^{-9} \text{ Hz}} \right)^{2/3} \text{ [Mpc]}$$

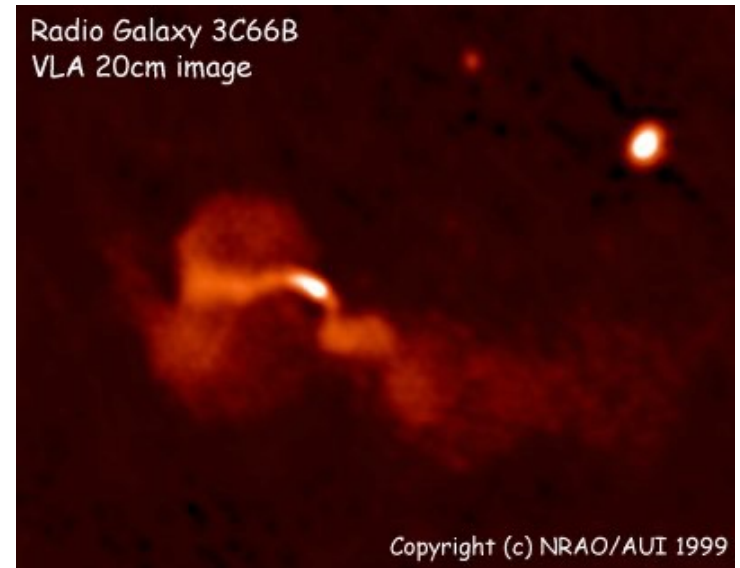
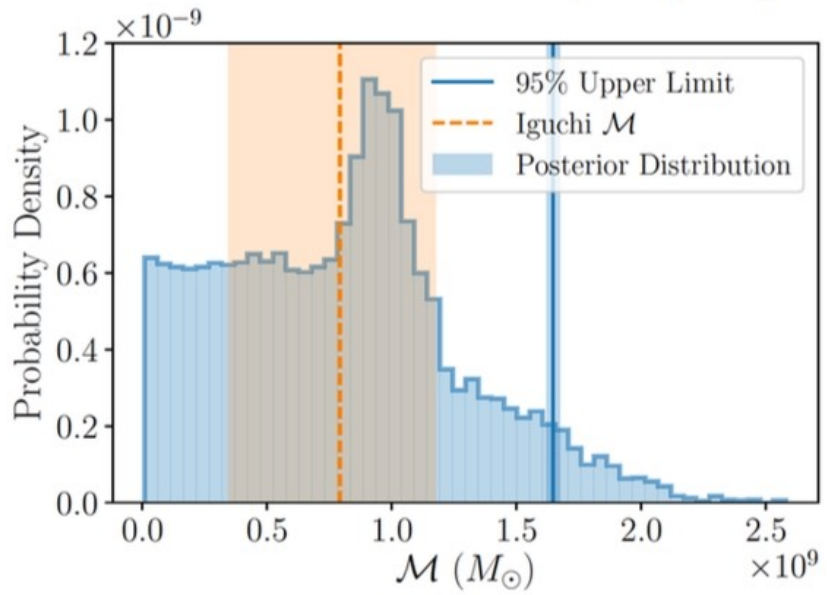


No Virgo SMBHBs with  $M > 1.6 \times 10^9$  solar masses.

# Targeted GW Searches

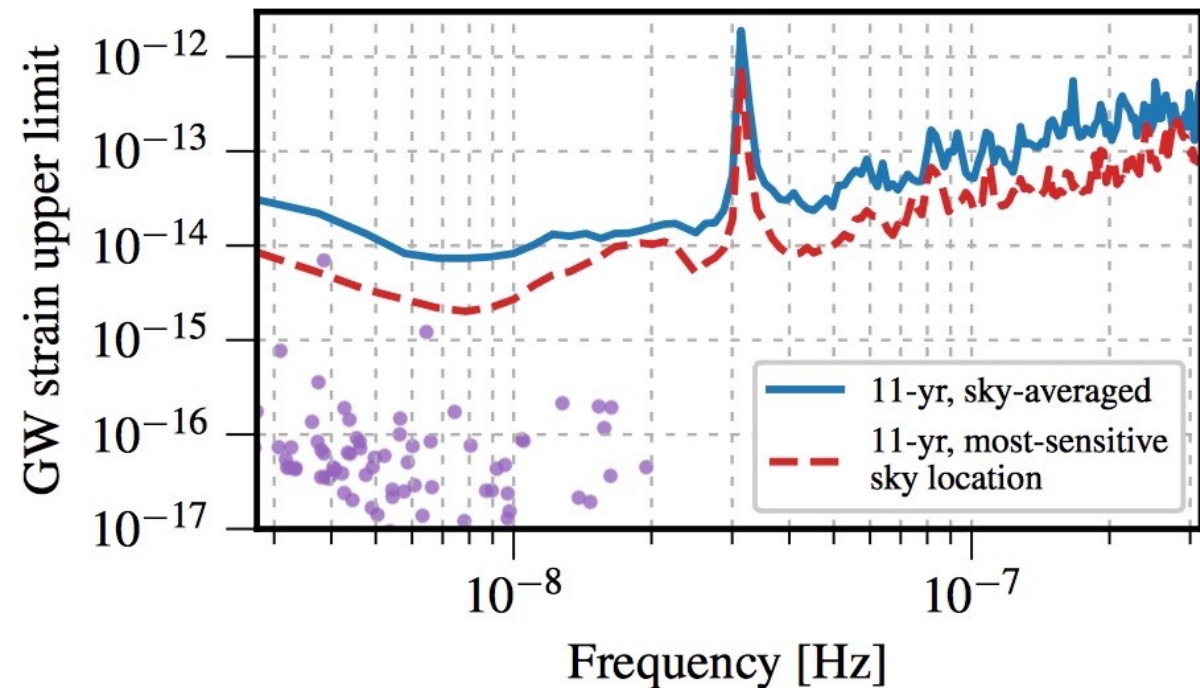
Nearby (85 Mpc) galaxy which shows evidence for binary black hole at core.

First mass estimates revised due to previous GW non-detections (Jenet et al. 2004).



Our current limit is getting very close to the published mass estimate.

# Continuous Wave Detection



A simulated realization of the local universe based on galaxies detected by 2MASS. In 34 out of 75,000 simulations single sources are detectable.

We expect a detection within next 10 years.

The NANOGrav Collaboration, 2019, ApJ, 880 116 and Mingarelli et al. 2018, Nature Astronomy, 1, 886

# Want to get there faster?

$$SNR \propto N_{\text{MSP}} T^{1/2} \left( \frac{c}{\sigma_{\text{RMS}}^2} \right)^{3/26} \quad \text{Siemens et al. 2013}$$

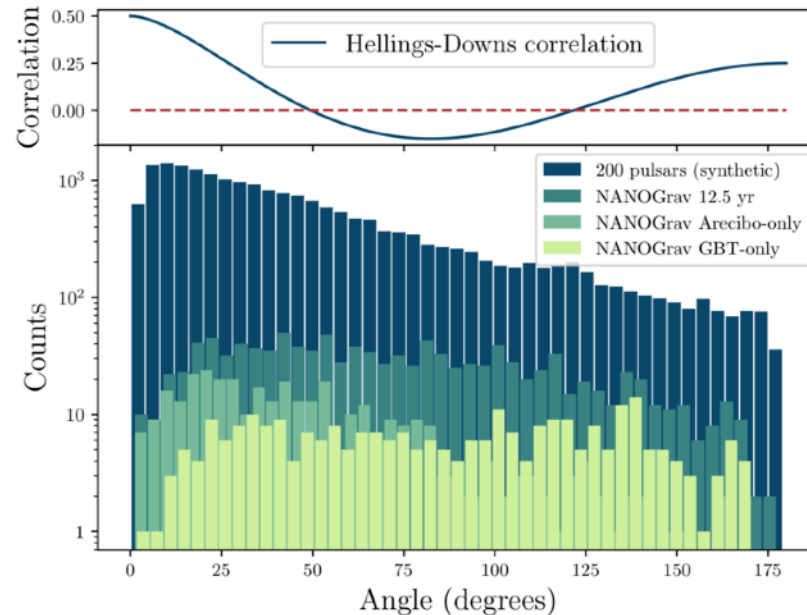
We need *more pulsars (in the right places)*, higher cadences, better timing precisions (bigger telescopes and bandwidths).

For single sources, cadence and precision are more important.

(+ *better ISM mitigation, noise characterization, ephemerides, etc.*)

# Going Forward

Increase to 200 MSPs by 2030.



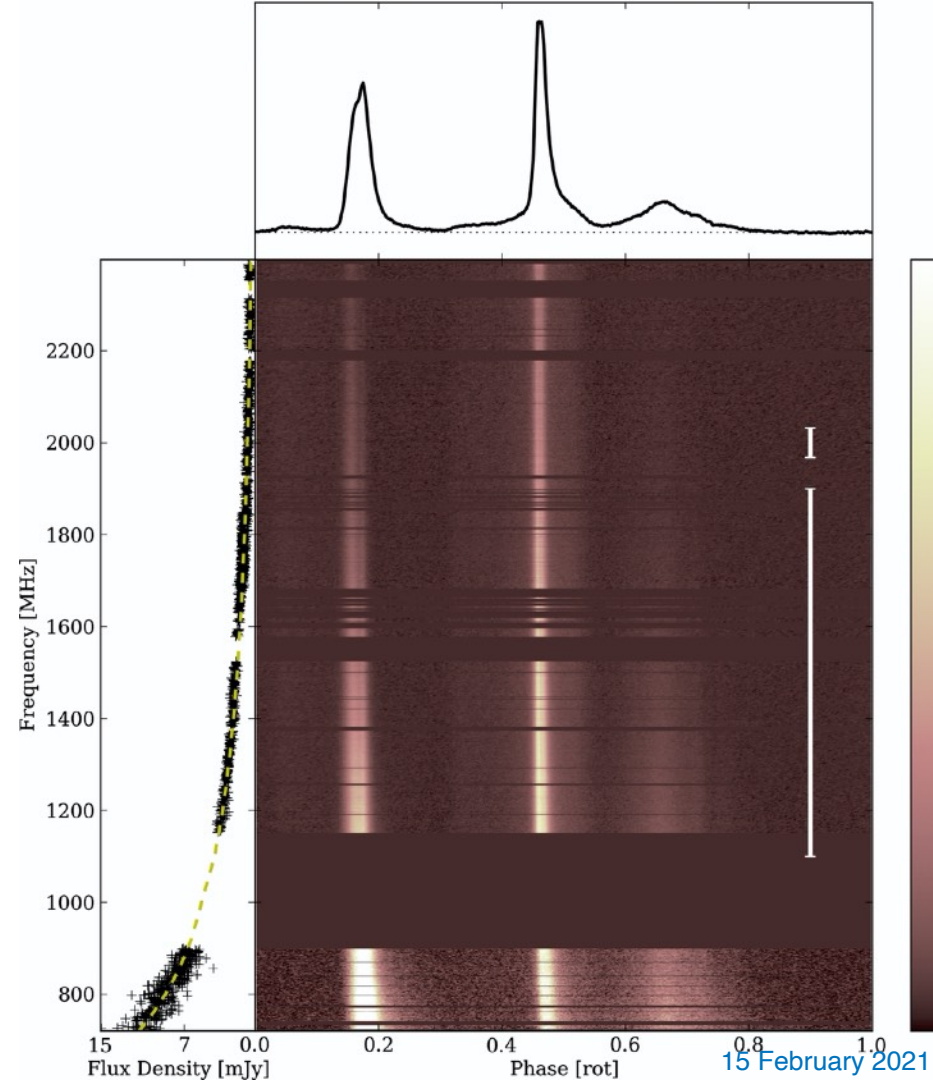
Ransom et al., 2019, NANOGrav  
Decadal Whitepaper, arXiv: 1908.05356

# Going Forward

Increase to 200 MSPs by 2030.

Develop a wideband receivers for the GBT.

Pennucci et al. 2014, ApJ, 790, 93



# Going Forward

Increase to 200 MSPs by 2030.

Develop a wideband receivers for the GBT.

Incorporate CHIME data.





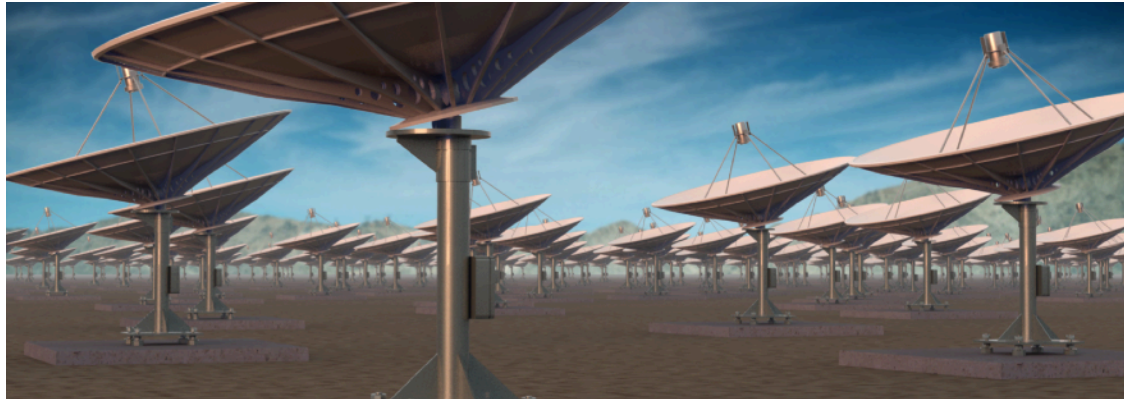
# Going Forward

Increase to 200 MSPs by 2030.

Develop a wideband receivers for the GBT.

Incorporate CHIME data.

Contribute to the development of next generation radio arrays.

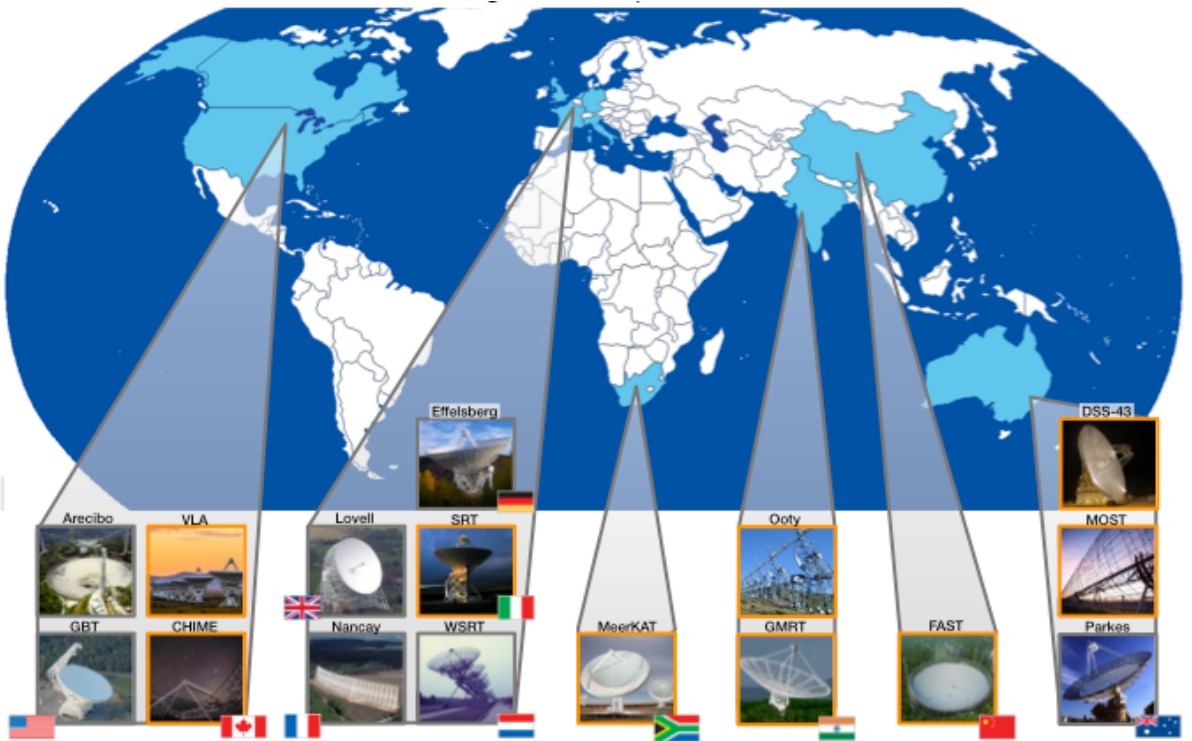


Hallinan, Ravi, et al.,  
2019, DSA-2000  
Decadal Whitepaper,  
arXiv:1907.07648

# The Expanded IPTA

Will soon be using 16 telescopes in 11 countries, bringing China, India, and South Africa into the collaboration.

This will be the most sensitive dataset in the world for low-frequency GW detection.



Credit: Shami Chatterjee

# Summary

- We are currently timing 40 MSPs with Green Bank and the VLA and hope to increase our GBT observation to compensate for loss of Arecibo.
- Our 12.5-yr dataset shows strong evidence for a common noise process consistent with gravitational waves. Spatial correlations should be detectable in our 15-yr dataset.
- Measurement of the amplitude and spectrum will provide unique insights into galaxy formation and evolution.
- Sensitivity has increased dramatically due to additional pulsars and improved instrumentation. Will continue to increase with even more pulsars, wider bandwidths, and **continued telescope access**.
- Looking to the future, new telescopes – most likely a large N, small D array – will be needed to characterize the low-frequency GW universe.